Inorganic Chemistry

Article

pubs.acs.org/IC

Hydroxide-Free Cubane-Shaped Tetranuclear [Ln_4] Complexes

Sourav Das,[†] Atanu Dey,[†] Sourav Biswas,[†] Enrique Colacio,*[,‡] and Vadapalli Chandrasekhar*[,†,§]

[†]Department of Chemistry, Indian Institute of Technology Kanpur, Kanpur-208016, India

[‡]Departamento de Química Inorgánica, Facultad de Ciencias, Universidad de Granada, Avenida de Fuentenueva s/n, 18071 Granada, Spain

[§]National Institute of Science Education and Research, Institute of Physics Campus, Sachivalaya Marg, PO: Sainik School, Bhubaneswar - 751 005, India

Supporting Information

ABSTRACT: The reaction of the lanthanide(III) chloride salts [Gd(III), Tb(III), and Dy(III)] with a new chelating, flexible, and sterically unencumbered multisite coordinating compartmental Schiff-base ligand (*E*)-2-((6-(hydroxymethyl)pyridin-2-yl)methyleneamino)phenol (LH_2) and pivalic acid (PivH) in the presence of triethylamine (Et_3N) affords a series of tetranuclear Ln(III) coordination compounds, $[Ln_4(L)_4(\mu_2\text{-}\eta^1\eta^1Piv)_4]\cdot xH_2O\cdot yCH_3OH$ (**1**, Ln = Gd(III), x = 3, y = 6; **2**, Ln = Tb(III), x = 6, y = 2; **3**, Ln = Dy(III), x = 4, y = 6). X-ray diffraction studies reveal that the molecular structure contains a distorted cubane-like $[Ln_4(\mu_3\text{-}OR)_4]^{+8}$ core, which is formed by the concerted coordination action of four dianionic L^{2-} Schiff-base ligands. Each lanthanide ion is eight-coordinated (2N, 6O) to form a distorted-triangular dodecahedral geometry. Alternating current susceptibility measurements of complex **3** reveal frequency- and temperature-dependent two-step out-of-phase signals under zero direct current (dc) field, which is characteristic of single-molecule magnet behavior. Analysis of the dynamic magnetic data under an applied dc field of 1000 Oe to fully or partly suppress the quantum tunneling of magnetization relaxation process affords the anisotropic barriers and pre-exponential factors: Δ/k_B = 73(2) K, $\tau_0 = 4.4 \times 10^{-8}$ s; Δ/k_B = 47.2(9) K, $\tau_0 = 5.0 \times 10^{-7}$ s for the slow and fast relaxations, respectively.

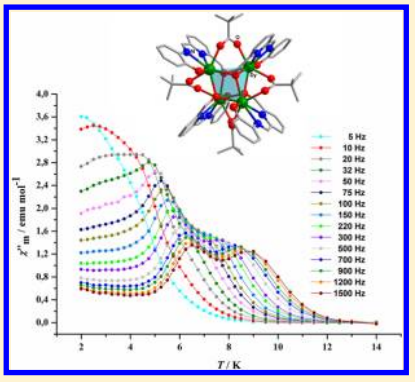

INTRODUCTION

Single-molecule magnets (SMMs) have been attracting interest from several points of view. Their potential applications in high-density information storage and processing, quantum computation, molecular spintronics,[1] and molecular refrigeration[2] are important factors that have motivated study of these systems. More importantly, however, the fundamental physics that is at the bottom of this behavior has intrigued and spurred intense interdisciplinary research in this area.[3] From a chemist's point of view, the interest in this field has been to utilize the understanding of the factors responsible for SMM behavior and create molecular ensembles that would behave as molecular magnets. The two important factors that seem to be directly responsible for SMM properties are the spin ground state (S) and uniaxial Ising-like anisotropy (D), which lead to an energy barrier of U [where $U = |D|S^2$ for an integer spin and $U = |D|(S^2 - 1/4)$ for a noninteger spin].[4] Chemically these two ingredients (S and D) can be achieved by different strategies. Polynuclear transition-metal complexes, under favorable geometric situations, can possess large ground-state spin values. Thus, the first SMM, $[Mn^{III}_8Mn^{IV}_4O_{12}(O_2CMe)_{16}(H_2O)_4]$[5], containing an inner core of 4 Mn^{4+} and an outer ring of 8 Mn^{3+}, has a ground-state spin of S = 10. The highest ground-state spin achieved thus far is by the complex $[Mn^{III}_{12}Mn^{II}_7(\mu_4\text{-}O)_8(\mu_3,\eta^1\text{-}N_3)_8(HL)_{12}(MeCN)_6]Cl_2\cdot 10MeOH\cdot MeCN$[6] ($H_3L$ = 2,6-bis(hydroxymethyl)-4-methylphenol), where S = 83/2. However, the mere fact that the latter possesses a high ground-state spin does not lend it the SMM behavior. On substitution of a central Mn(II) by a Dy(III) ion in the compound $[Mn^{III}_{12}Mn^{II}_6Dy^{III}(\mu_4\text{-}O)_8(\mu_3\text{-}Cl)_{6.5}(\mu_3\text{-}N_3)_{1.5}(HL)_{12}(MeOH)_6]Cl_3\cdot 25MeOH$[7] ($H_3L$ = 2,6-bis(hydroxymethyl)-4-methylphenol), the latter complex displays SMM behavior. Such experiments, focusing on the magnetic anisotropy of lanthanide ions, have created a lot of interest in lanthanide complexes of varying nuclearity.[8] On the basis of such studies, it is now known that lanthanide complexes can also function as mononuclear SMMs[9] as first shown by Ishikawa's double-decker complex, $[Pc_2Tb]^-$.[9a] The importance of homonuclear lanthanide complexes in molecular magnetism has increased since the discovery that $\{Dy_5\}$[10] and $\{Dy_4K_2\}$[11] complexes show the highest barriers of energy for reversal of magnetization in any system so far. We have been interested in homo-[12] and heterometallic[13] systems in general and in their utility in molecule-based magnets in particular. Among the structural topologies that have been investigated for polynuclear metal complexes, cubane cores are well-known among transition-metal complexes[14] but are much less investigated with the lanthanide ions,[15] particularly because these syntheses are challenging. Not surprisingly, thus far, there have been only a

Received: November 12, 2013
Published: March 27, 2014

   dx.doi.org/10.1021/ic402827b | *Inorg. Chem.* 2014, 53, 3417−3426

Table 1. Crystal Data and Structure Refinement Parameters of Complexes 1−3

	1	2	3
formula	$C_{78}H_{104}N_8O_{25}Gd_4$	$C_{74}H_{84}N_8O_{24}Tb_4$	$C_{78}H_{100}Dy_4N_8O_{26}$
M/g	2182.69	2105.17	2215.66
crystal system	monoclinic	monoclinic	monoclinic
space group	$P2_1/c$	$P2_1/c$	$P2_1/c$
a/Å	18.788(5)	17.781(3)	18.644(5)
b/Å	16.882(5)	17.155(3)	16.890(5)
c/Å	27.893(5)	26.846(4)	28.125(5)
β (deg)	102.470(5)	100.194(3)	103.149(5)
V/Å^3	8638(4)	8060(2)	8624(4)
Z	4	4	4
ρ_c/g cm^{-3}	1.678	1.735	1.706
μ/mm^{-1}	3.109	3.546	3.505
F(000)	4336	4144	4384
cryst size (mm^3)	0.056 × 0.038 × 0.021	0.056 × 0.042 × 0.037	0.052 × 0.036 × 0.019
θ range (deg)	4.09 to 25.03	4.13 to 25.03	2.04 to 25.50
limiting indices	$-22 \le h \le 22$	$-21 \le h \le 11$	$-22 \le h \le 22$
	$-20 \le k \le 10$	$-20 \le k \le 20$	$-20 \le k \le 19$
	$-33 \le l \le 33$	$-31 \le l \le 31$	$-27 \le l \le 34$
reflns collected	44 268	45 166	60 389
ind reflns	15 167 [R(int) = 0.0784]	14 155 [R(int) = 0.0578]	16 064 [R(int) = 0.0835]
completeness to θ (%)	99.5	99.5	99.9
refinement method	full-matrix least-squares on F^2	full-matrix least-squares on F^2	full-matrix least-squares on F^2
data/restraints/params	15 167/2/1060	14 155/0/1007	16 064/62/1051
goodness-of-fit on F^2	1.042	1.011	1.029
final R indices	R_1 = 0.0718	R_1 = 0.0398	R_1 = 0.0571
[$I > 2\theta(I)$]	wR_2 = 0.1655	wR_2 = 0.0911	wR_2 = 0.1423
R indices (all data)	R_1 = 0.1073	R_1 = 0.0629	R_1 = 0.0942
	wR_2 = 0.1860	wR_2 = 0.1010	wR_2 = 0.1632
largest diff. peak and hole (e·Å^{-3})	1.920 and −1.145	2.357 and −1.428	2.636 and −1.725

few such examples whose magnetism has been properly investigated, such as $[Dy_4(\mu_3\text{-}OH)_4(isonicotinate)_6(py)(CH_3OH)_7](ClO_4)_2\cdot py\cdot 4CH_3OH$,[15a] $[Dy_4(HL)_4(C_6H_4NH_2COO)_2(\mu_3\text{-}OH)_4(\mu\text{-}OH)_2(H_2O)_4]\cdot 4CH_3CN\cdot 12H_2O$[15b] (where LH_2 = 2-{[(2-hydroxy-3-methoxyphenyl)-methylidene]amino}benzoic acid), and $[Ln_4(OH)_4(TBSOC)_2(H_2O)_4(CH_3OH)_4]\cdot 4H_2O$[15c] ($H_4TBSOC$ = *p-tert*-butylsulfonylcalix[4]arene; Ln = Dy, Ho). We report, herein, a new chelating, flexible, and sterically unencumbered multisite coordinating compartmental Schiff-base ligand, (*E*)-2-((6-(hydroxymethyl)pyridin-2-yl)methyleneamino)phenol (LH_2). Using this ligand, we were able to assemble a series of neutral tetranuclear cubane-shaped {Ln(III)}$_4$ complexes (Ln = Gd, Tb, and Dy). Magnetic studies on these complexes revealed that the Dy(III) analogue is an SMM. Unlike the previous examples reported, the current family of cubane-shaped tetranuclear Ln_4 ensembles do not possess bridging hydroxide ligands.

EXPERIMENTAL SECTION

Solvents and other general reagents used in this work were purified according to standard procedures.[16] 2,6-Bis(hydroxymethyl)pyridine (**C1**), activated manganese(IV) dioxide (MnO_2), $DyCl_3\cdot 6H_2O$, $TbCl_3\cdot 6H_2O$, and $GdCl_3\cdot 6H_2O$ were obtained from Sigma Aldrich Chemical Co. and were used as received. 2-Aminophenol and sodium sulfate (anhydrous) were obtained from SD Fine Chemicals, Mumbai, India and were used as such. 6-Hydroxymethyl-2-pyridinecarboxaldehyde (**C2**) was prepared according to a literature procedure.[17]

Instrumentation. Melting points were measured using a JSGW melting point apparatus and are uncorrected. IR spectra were recorded as KBr pellets on a Bruker Vector 22 FT-IR spectrophotometer operating at 400−4000 cm^{-1}. Elemental analyses of the compounds were obtained from Thermoquest CE instruments CHNS-O, EA/110 model. ^{1}H NMR spectra were recorded in $CDCl_3$ solutions on a JEOL JNM LAMBDA 400 model spectrometer operating at 400 MHz; chemical shifts are reported in parts per million (ppm) and are referenced with respect to internal tetramethylsilane (^{1}H).

Magnetic Measurements. Field dependence of the magnetization at different temperatures and variable temperature (2−300 K) magnetic susceptibility measurements on polycrystalline samples were carried out with a Quantum Design SQUID MPMS XL-5 device operating at different magnetic fields. Alternating current (ac) susceptibility measurements were performed using an oscillating ac field of 3.5 Oe and ac frequencies ranging from 1 to 1500 Hz. The experimental susceptibilities were corrected for the sample holder and diamagnetism of the constituent atoms by using Pascal's tables. A pellet of the sample cut into very small pieces was placed in the sample holder to prevent any torquing of the microcrystals.

X-ray Crystallography. The crystal data for the compounds were collected on a Bruker SMART CCD diffractometer (Mo Kα radiation, λ = 0.710 73 Å). The program SMART[18a] was used for collecting frames of data, indexing reflections, and determining lattice parameters; the SAINT[18a] program was used for integration of the intensity of reflections and scaling; the SADABS[18b] program was used for absorption correction; and the SHELXTL[18c,d] program was used for space group, structure determination, and least-squares refinements on F^2. All the structures were solved by direct methods using the program SHELXS-97[18e] and refined by full-matrix least-squares methods against F^2 with SHELXL-97.[18e] Hydrogen atoms were fixed at calculated positions, and their positions were refined by a riding model. All the non-hydrogen atoms were refined with anisotropic displacement parameters. The crystallographic figures were generated using Diamond 3.1e software.[18f] The crystal data and the cell parameters for compounds **1**−**3** are summarized in Table 1.

dx.doi.org/10.1021/ic402827b | Inorg. Chem. 2014, 53, 3417−3426

Synthesis. *(E)-2-((6-(Hydroxymethyl)pyridin-2-yl)-methyleneamino)phenol (LH_2).* To a stirred solution of **C2** (1.50 g, 10.93 mmol) in dry methanol (20 mL), 2-aminophenol (1.19 g, 10.93 mmol), also dissolved in dry methanol (20 mL), was added dropwise over a period of 15 min, and the resulting reaction mixture was stirred for 24 h under N_2 atmosphere at room temperature. Then, the solvent was concentrated in vacuo to 10 mL and kept in a refrigerator at 0 °C for 5 h to get a reddish brown solid. Yield: 2.10 g, 84.16%. Mp: 116 °C. Fourier transform infrared (FT-IR) (KBr) cm^{-1}: 3061 (b), 2914 (m), 2841 (m), 1627 (m), 1585 (s), 1486 (s), 1445 (s) 1372 (s), 1336 (s), 1299 (s), 1226 (s), 1200 (s), 1137(s), 1089(m), 1031(m), 954(m). ^1H NMR ($CDCl_3$, δ, ppm): 8.77 (s, 1H, imino), 8.03 (d, 1H, Ar−H), 7.82 (t, 1H, Py−H), 7.37 (d, 2H, Py−H), 7.25 (t, 1H, Ar−H), 7.03 (s, 1H, Ar−H), 6.93 (t, 1H, Ar−H), 4.83 (s, 2H, CH_2OH). Anal. Calcd for $C_{13}H_{12}N_2O_2$: C, 68.41; H, 5.30; N, 12.27 Found: C, 68.30; H, 5.28; N, 12.19%.

*General Synthetic Procedure for the Preparation of Complexes **1**−**3**.* All the metal complexes (**1**−**3**) were synthesized according to the following procedure. Ligand LH_2 (0.06 g, 0.26 mmol) was dissolved in methanol (10 mL). To this solution, $LnCl_3{\cdot}6H_2O$ (0.26 mmol) was added, and the reaction mixture was stirred at room temperature for 10 min. At this stage triethylamine (0.09 g, 0.9 mmol) was added dropwise to this solution. Then, pivalic acid (PivH) (0.026 g, 0.26 mmol) was added to the mixture, which was stirred for a further period of 6 h at room temperature to afford a reddish precipitate, which was washed with diethyl ether, dried, and redissolved in chloroform/methanol (1:1) and kept for crystallization. After about 10 d, block-shaped red crystals suitable for X-ray crystallography were obtained by slow evaporation of the solvent mixture. Specific details of each reaction and the characterization data of the products obtained are given below.

*$[Gd_4(L)_4(\mu_2\text{-}\eta^1\eta^1Piv)_4]{\cdot}6CH_3OH{\cdot}3H_2O$ (**1**).* Quantities: LH_2 (0.06 g, 0.26 mmol), $GdCl_3{\cdot}6H_2O$ (0.097 g, 0.26 mmol), Et_3N (0.12 mL, 0.9 mmol), PivH (0.026 g, 0.26 mmol). Yield: 0.072 g, 51.07% (based on Gd). Mp: 183 °C (dec). IR (KBr) cm^{-1}: 3389(b), 3060(w), 2959(s), 1586(s), 1574(s), 1477(s), 1421(s), 1374(s), 1361(s), 1288(s), 1225(w), 1180(w), 1151(s), 1016(w), 930(w), 874(w), 829(s). Anal. Calcd for $C_{78}H_{106}N_8O_{25}Gd_4$ (2186.42): C, 42.88; H, 4.89; N, 5.13. Found: C, 42.79; H, 4.91; N, 5.23%.

*$[Tb_4(L)_4(\mu_2\text{-}\eta^1\eta^1Piv)_4]{\cdot}2CH_3OH{\cdot}6H_2O$ (**2**).* Quantities: LH_3 (0.06 g, 0.26 mmol), $TbCl_3{\cdot}5H_2O$ (0.097 g, 0.26 mmol), Et_3N (0.12 mL, 0.9 mmol), PivH (0.026 g, 0.26 mmol). Yield: 0.075 g, 54.8% (based on Tb). Mp: 185 °C (dec). IR (KBr) (cm^{-1}): 3395(b), 3060(w), 2959(s), 1587(s), 1574(s), 1556(s), 1478(s), 1421(s), 1375(s), 1361(s), 1289(s), 1226(w), 1181(w), 1152(s), 1017(w), 934(w), 860(w). Anal. Calcd for $C_{74}H_{96}N_8O_{24}Tb_4$ (2116.36): C, 41.98; H, 4.57; N, 5.29. Found: C, 42.10; H, 4.36; N, 5.38%.

*$[Dy_4(L)_4(\mu_2\text{-}\eta^1\eta^1Piv)_4]{\cdot}6CH_3OH{\cdot}4H_2O$ (**3**).* Quantities: LH_3 (0.06 g, 0.26 mmol), $DyCl_3{\cdot}5H_2O$ (0.097 g, 0.26 mmol), Et_3N (0.12 mL, 0.9 mmol), PivH (0.026 g, 0.26 mmol). Yield: 0.071 g, 49.30% (based on Dy). Mp: 185 °C (dec). IR (KBr) (cm^{-1}): 3392(b), 3062(w), 2959(s), 1587(s), 1575(s), 1559(s), 1477(s), 1421(s), 1374(s), 1361(s), 1290(s), 1225(w), 1180(w), 1112(w), 1016(s), 928(w), 854(w). Anal. Calcd for $C_{78}H_{108}N_8O_{26}Dy_4$ (2228.45): C, 42.13; H, 4.90; N, 5.04. Found: C, 42.01; H, 4.79; N, 5.13%.

RESULTS AND DISCUSSION

Synthesis. The multisite coordinating Schiff-base ligand LH_2 was prepared by a two-step synthetic protocol involving the conversion of the precursor **C1** to **C2**, which was subsequently condensed with 2-amino phenol (Scheme 1). Ligand LH_2 contains four divergent coordinating centers: a phenolic unit, an imino, a pyridine nitrogen, and a pendant CH_2OH arm. We expected this semiflexible unsymmetrical Schiff-base ligand to accommodate one lanthanide metal ion. However, the presence of the $-CH_2OH$ arm was expected to allow the assembly to proliferate. We used pivalic acid as a coligand because of the propensity of the pivalate ion to bridge adjacent metal centers.[12b,19] Accordingly, the reaction of LH_2, $LnCl_3{\cdot}nH_2O$, and pivalic acid (in a 1:1:1 stoichiometric ratio, in the presence of 4 equiv of triethylamine as the base) in methanol/chloroform (1:1) allowed the formation of neutral tetranuclear Ln(III) complexes **1**−**3**, $[Ln_4(L)_4(\mu_2\text{-}\eta^1\eta^1Piv)_4]{\cdot}xH_2O{\cdot}yCH_3OH$ (**1**, Ln = Gd(III), x = 3, y = 6; **2**, Ln = Tb(III), x = 6, y = 2; **3**, Ln = Dy(III), x = 4, y = 6), which were shown to be present in a distorted cubane-type topology (see Scheme 2).

Scheme 1. Synthesis of LH_2

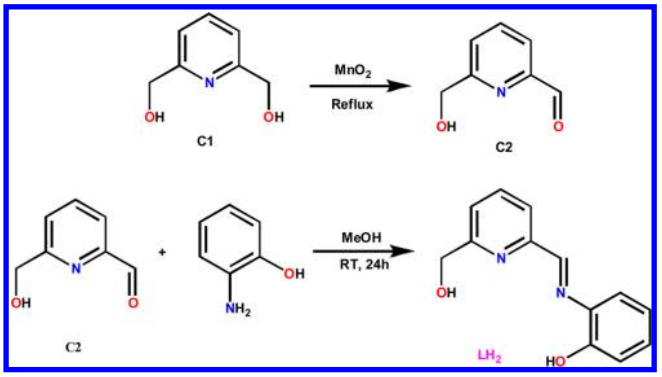

X-ray Crystal Structures of Compounds 1−3. Single-crystal X-ray diffraction studies reveal that compounds **1**−**3** are isostructural and crystallize in the monoclinic space group $P2_1/c$ with Z = 4. All the compounds are neutral and have the same structural topology, namely, a distorted cubane-type tetrametallic core. In view of their structural similarity, only the

Scheme 2. Synthesis of Compounds 1−3

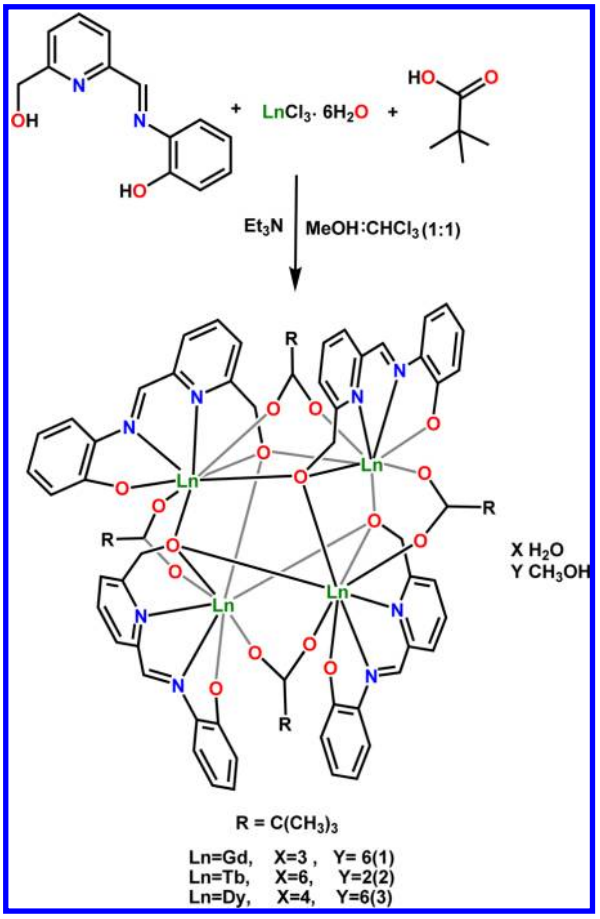

dx.doi.org/10.1021/ic402827b | Inorg. Chem. 2014, 53, 3417−3426

Table 2. Selected Bond Distance (Å) and Bond Angle (deg) Parameters of Compound 3

Dy(1)−O(2)	2.273(7)	Dy(2)−Dy(3)	3.707 (9)	Dy(1)−O(1)−Dy(2)	100.4(2)
Dy(1)−O(9)	2.305(7)	Dy(3)−O(6)	2.272(7)	Dy(1)−O(1)−Dy(4)	99.3(2)
Dy(1)−O(16)	2.325(7)	Dy(3)−O(12)	2.315(7)	Dy(2)−O(1)−Dy(4)	114.1(3)
Dy(1)−O(1)	2.370(7)	Dy(3)−O(13)	2.325(7)	Dy(2)−O(3)−Dy(3)	100.2(2)
Dy(1)−O(7)	2.472(6)	Dy(3)−O(5)	2.361(7)	Dy(2)−O(3)−Dy(1)	100.0(2)
Dy(1)−O(3)	2.491(7)	Dy(3)−O(3)	2.466(6)	Dy(3)−O(3)−Dy(1)	113.9(2)
Dy(1)−N(1)	2.501(8)	Dy(3)−O(7)	2.481(7)	Dy(3)−O(5)−Dy(2)	100.2(2)
Dy(1)−N(2)	2.548(9)	Dy(3)−N(5)	2.496(8)	Dy(3)−O(5)−Dy(4)	99.3(2)
Dy(1)−Dy(4)	3.708(11)	Dy(3)−N(6)	2.530(8)	Dy(2)−O(5)−Dy(4)	115.1(2)
Dy(1)−Dy(2)	3.721(10)	Dy(3)−Dy(4)	3.684(8)	Dy(4)−O(7)−Dy(1)	100.3(2)
Dy(2)−O(4)	2.263(7)	Dy(4)−O(8)	2.254(7)	Dy(4)−O(7)−Dy(3)	99.2(2)
Dy(2)−O(10)	2.353(7)	Dy(4)−O(14)	2.323(7)	Dy(1)−O(7)−Dy(3)	114.1(2)
Dy(2)−O(11)	2.359(7)	Dy(4)−O(15)	2.331(7)		
Dy(2)−O(3)	2.367(7)	Dy(4)−O(7)	2.357(7)		
Dy(2)−O(5)	2.470(6)	Dy(4)−O(5)	2.474(7)		
Dy(2)−O(1)	2.475(7)	Dy(4)−N(7)	2.493(8)		
Dy(2)−N(3)	2.476(9)	Dy(4)−O(1)	2.495(7)		
Dy(2)−N(4)	2.524(8)				

molecular structure of **3** will be described; the structural details of **1**−**2** are given in the Supporting Information (Figures S1 and S2). Selected bond parameters of **3** are summarized in Table 2. The molecular structures and selected bond parameters of the other two compounds are given in the Supporting Information (Figures S1 and S2, Tables S1 and S2). A perspective view of the molecular structure of **3** is depicted in Figure 1.

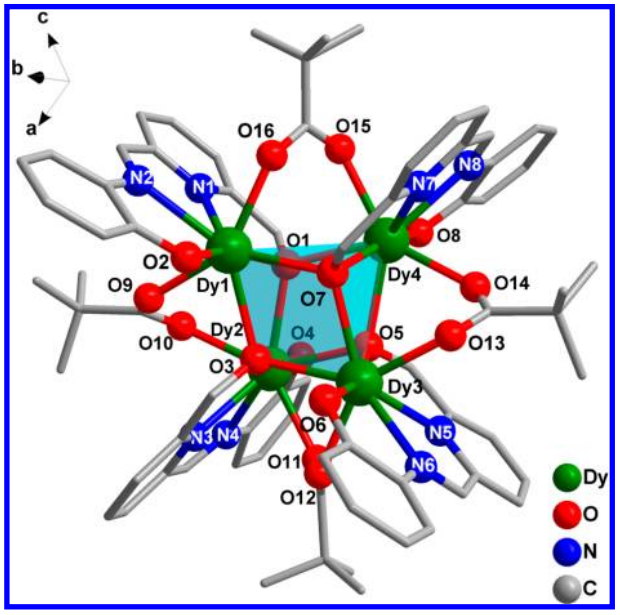

Figure 1. Molecular structure of **3** (hydrogen atoms and the solvent molecules have been omitted for clarity).

The molecular structure of **3** (Figures 1 and 2a) contains a distorted cubane-like $[Dy_4(\mu_3\text{-}OR)_4]^{+8}$ core, which is formed by the concerted coordination action of four dianionic L^{2-} Schiff-base ligands in a $\mu_3\text{-}\eta^3\text{:}\eta^1\text{:}\eta^1\text{:}\eta^1$ fashion. Here, each ligand provides one phenolate oxygen, one imino nitrogen, one pyridine nitrogen, and one μ_3-alkoxy oxygen group (Scheme 3). Potentially, each ligand can accommodate one Dy(III) in its chelating (O, N, N, O) cavity. Thus, in compound **3**, four $Dy(L)^+$ building units are self-assembled through fully deprotonated alkoxy oxygen atoms. The latter are involved in bridging three neighboring Dy(III) ions [$Dy-O_{alkoxy}$ = 2.36−2.49 Å] to construct a distorted cubane-like $[Dy_4(\mu_3\text{-}OR)_4]^{+8}$ core (Figures 1 and 2a). Within the core, the intramolecular Dy···Dy distances are in the range of 3.68−4.15 Å. In addition to the binding provided by L^{2-}, all the Dy(III) ions in the Dy_4 cubane core are further held together as a result of four $\mu_2\text{-}\eta^1\text{:}\eta^1$ binding of pivalate anion, which satisfies the charge as well as the coordination environment. Each pivalate ligand is involved in a syn, syn bridge among all adjacent Dy(III) ions with an average distance of 2.31−2.35 Å. Each dysprosium ion is eight-coordinated (2N, 6O) and forms distorted triangular dodecahedral geometry (Figure 2b and SHAPE[20] calculations in the Supporting Information).

The $Dy-O_{phenoxy}$ bond lengths are in the range of ∼2.25−2.27 Å, which are slightly shorter than $Dy-O_{alkoxy}$ bond lengths (∼2.36−2.49 Å). Two different types of nitrogens are coordinated to each Dy(III) ions. Bond lengths of coordinated imino nitrogens are in the range of ∼2.52−2.54 Å, which are slightly longer than those of pyridine ring nitrogen [$Dy-N_{Pyridine}$ = 2.47−2.49 Å]. The Dy−O−Dy angles lie in rather wide ranges: 99.20(2)−115.10(2)°. The bond lengths around the lanthanide ions show almost the expected general tendency toward shorter values over the series **1**, **2**, and **3**, which is consistent with the phenomenon of lanthanide contraction (Table 3).

As pointed out above, there are only three discrete Dy_4 complexes possessing distorted cubane geometries whose magnetic properties have been well explored and are known in the literature. These are illustrated in Figure 3. In these cases, the corners of the cubane are occupied by Dy and μ_3-OH^- ions. In the current instance, in contrast, the oxygen atom $(-CH_2O)^-$ present in the vertex of the cube is derived from the ligand $[L]^{2-}$. The metric parameters involved in the current instance are similar to those found in the literature and are summarized in Table 4.

Magnetic Studies. The temperature dependence of $\chi_M T$ for complexes **1**−**3** (χ_M is the molar magnetic susceptibility per Ln_4^{III} unit) in the temperature range of 300−2 K was measured with an applied magnetic field of 1000 Oe, and the results are displayed in Figure 4.

dx.doi.org/10.1021/ic402827b | Inorg. Chem. 2014, 53, 3417−3426

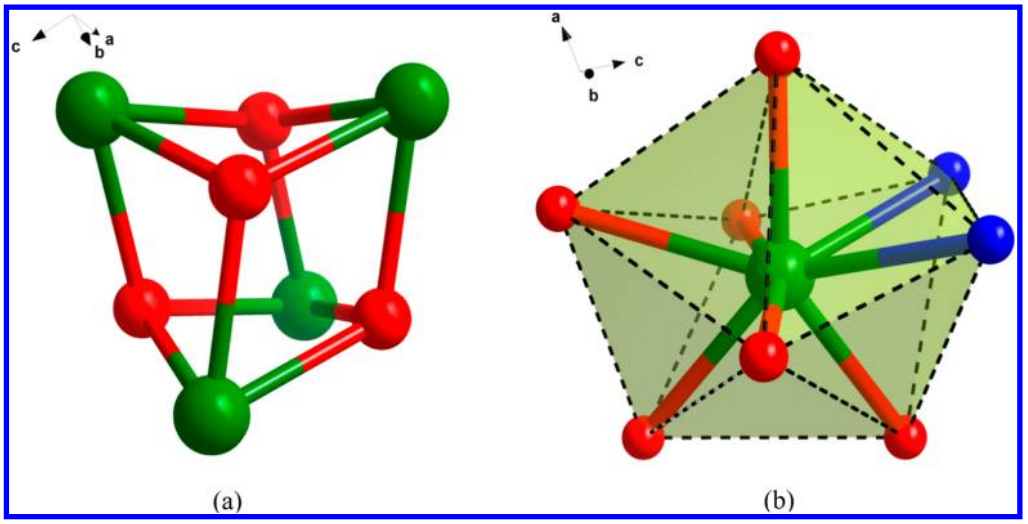

Figure 2. (a) Distorted cubane core of complex **3**. (b) Distorted triangular dodecahedral geometry around Dy^{3+} ion.

Scheme 3. Binding Mode of the Ligand $[L]^{2-}$ with Dysprosium(III) Ions

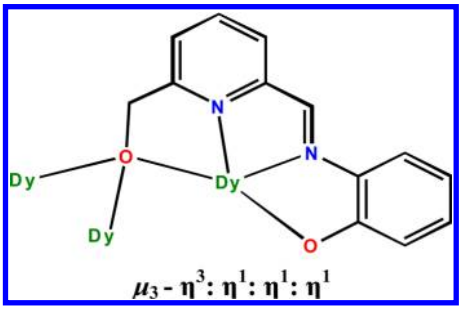

Let us start with the simple case of the Gd_4^{III} complex **1**. At room temperature, the $\chi_M T$ value for **1** of 32.42 cm^3 mol^{-1} K is close to that expected for four noninteracting Gd^{III} ions (31.5 cm^3 mol^{-1} K, with $S = 7/2$ and $g = 2$). On lowering the temperature, the $\chi_M T$ for **1** remains constant until ~25 K and then shows an abrupt decrease to reach a value of 15.91 cm^3 mol^{-1} K at 2 K. This behavior is most likely due to intramolecular antiferromagnetic interactions between the Gd^{III} ions.

The Gd_4O_4 cubane unit in **1** is of the 4 + 2 type with two long (~4.15 Å) and four short (~3.7 Å) Gd···Gd distances. In keeping with this, the magnetic properties of **1** were analyzed using following simplest two-J isotropic Hamiltonian:

$$H = -J_1(S_{Gd1}S_{Gd4} + S_{Gd1}S_{Gd2} + S_{Gd2}S_{Gd3} + S_{Gd3}S_{Gd4}) - J_2(S_{Gd1}S_{Gd3} + S_{Gd2}S_{Gd4})$$

where J_1 and J_2 describe the magnetic exchange pathways involving short and long Gd···Gd distances, respectively (Figure 4). The D_{Gd} is assumed to be negligible as this ion is rather isotropic. The fit of the experimental susceptibility data with the above Hamiltonian, using the MAGMUN program,[21] afforded the following set of parameters: $J_1 = -0.03$ cm^{-1}, $J_2 = -0.13$ cm^{-1}, $g = 2.03$, and $R = 3 \times 10^{-7}$ ($R = \Sigma(\chi_{obs}T - \chi_{calc}T)^2/\Sigma(\chi_{obs}T)^2$, where χ_{calc} and χ_{obs} denote calculated and observed molar magnetic susceptibilities, respectively). The obtained values are in good agreement with the reported coupling constants for other dialkoxo and diphenoxo-bridged Gd^{3+} complexes.[22,12b] The structural differences between the Gd_2O_2 bridging fragments involving short and long Gd···Gd distances could be responsible for the differing magnetic coupling of the two magnetic pathways. Thus, while the magnetic exchange pathways involving short Gd···Gd distances are folded (due to coordination of the nonplanar syn-syn pivalate bridging ligand), with Gd−O−Gd bridging angles of ~98°, those involving long Gd···Gd distances are planar, with Gd−O−Gd bridging angles of ~114°. Nevertheless, more examples of dialkoxo-bridged complexes are needed to evaluate the influence of the structural factors of the Gd_2O_2 bridging fragment on the magnetic coupling.

As expected for four noninteracting Gd^{3+} ions, the experimental magnetization values (Figure 5) are well below the Brillouin function, which is mainly due to the antiferromagnetic interaction between the metal ions as well as to the local magnetic anisotropy of the Gd^{3+} ions. The saturation of the magnetization is almost complete at 5 T, reaching a value of 28.34 $N\mu_B$, which agrees well with the theoretical saturation value for four Gd^{3+} ions with $g = 2.03$ of 28.42 $N\mu_B$.

The room-temperature $\chi_M T$ values of complexes **2** and **3** are 48.31 and 56.51 cm^3 mol^{-1} K, respectively, which are in rather good agreement with the expected theoretical values using the free ion approximation (47.28 and 56.72 cm^3 mol^{-1} K for **2** and

Table 3. Comparison of Selected Average Ln−O and Ln−N Bond Lengths (Å) of Compounds 1−3

	1 (Ln(III) = Gd(III))	**2** (Ln(III) = Tb(III))	**3** (Ln(III) = Dy(III))
$Ln-O_{phenolate}$	2.292(8)	2.285(4)	2.265(7)
$Ln-O_{alkoxy}$	2.463(7)	2.446(4)	2.439(7)
$Ln-O_{pivalate}$	2.365(8)	2.342(4)	2.329(7)
$Ln-N_{imine}$	2.559(10)	2.544(5)	2.533(8)
$Ln-N_{Py}$	2.515(10)	2.506(5)	2.491(8)

dx.doi.org/10.1021/ic402827b | Inorg. Chem. 2014, 53, 3417−3426

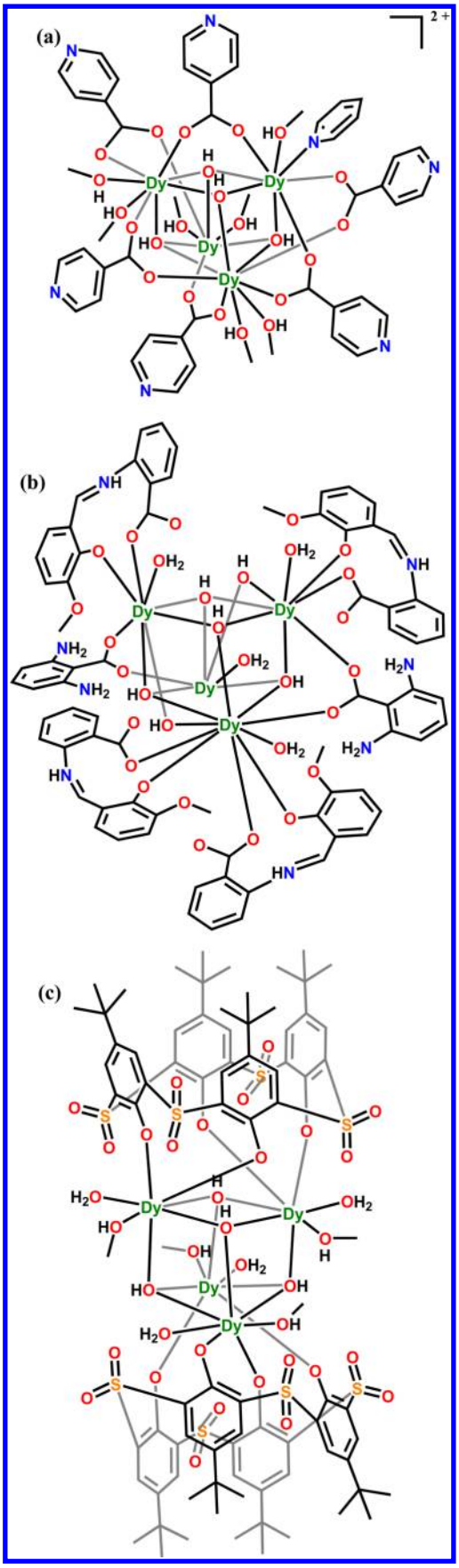

Figure 3. Examples of reported discrete tetranuclear lanthanide complexes having the cubane core.

3, respectively) for four noninteracting lanthanide ions: Tb^{3+} ($^7F_6$, $S = 3$, $L = 3$, $g = 3/2$, $C = 11.82$ cm^3 mol^{-1} K) and Dy^{3+} ($^6H_{15/2}$, $S = 5/2$, $L = 5$, $g = 4/3$, $C = 14$ cm^3 mol^{-1} K). The product χT decreases with decreasing temperature, first slowly to ~50 K for compound **2** and to ~100 K for compound **3** and then rapidly to 33.25 and 39.98 cm^3 mol^{-1} K at 2.0 K, respectively. This behavior is due to the effects of the thermal depopulation of the m_J sublevels of the $^{2S+1}\Gamma_J$ ground state of the Ln^{3+} ion, which are originated by the crystal field, together with weak $Ln^{3+}\cdots Ln^{3+}$ antiferromagnetic interactions. The existence of very weak antiferromagnetic interactions in theses complexes is not unexpected in view of the fact that isostructural Gd^{3+}, Tb^{3+}, and Dy^{3+} complexes generally display magnetic exchange interactions of the same nature.[23,13b]

The field dependence of the magnetization at 2 K shows a rapid increase of the magnetization at low field and a linear increase at high field to reach values of 23.5 and 24.47 $N\mu_B$ for compounds **2** and **3** (Figure 5), respectively, which are considerably smaller than the expected saturation magnetization values, $Ms/N\mu_B = 4g_JJ$, for four Ln^{3+} ions. This behavior suggests the presence of a significant magnetic anisotropy arising from the ligand-field effects, which eliminates the 16-fold degeneracy of the $^6H_{15/2}$ ground state. In fact, the observed values at 5 T per Ln^{3+} ion are similar to those estimated for mononuclear Ln^{3+} complexes where considerable ligand-field effects have been taken into account.[24]

Dynamic ac magnetic susceptibility measurements as a function of the temperature at different frequencies were performed on microcrystalline powder samples of complexes **2** and **3**. Complex **2** did not show any out-of-phase (χ''_M) signal, either under zero external field or under an applied field of 1000 Oe. This behavior indicates that either the energy barrier for the flipping of the magnetization is not high enough to trap the magnetization in one of the equivalent configurations above 2 K or there exists quantum tunnelling of the magnetization (QTM), leading to a flipping rate that is too fast to observe the maximum in the χ''_M above 2 K. Complex **3**, however, shows typical SMM behavior (Figure 6 and Supporting Information, Figure S3) below 13 K under zero dc applied field with two out-of-phase peaks in the 5.75 K (300)−6.25 K (1400 Hz) range (fast relaxation, FR) and 8.5 K (300 Hz)−10.5 K (1400 Hz) range (slow relaxation, SR). Note that the χ''_M component increases below the maxima of the FR process, which can be taken as a clear indication of QTM.

The Cole−Cole diagram (Figure 6, inset) exhibits a semicircular shape in the 3.75−9 K range, which is due to the coalescence of the FR and SR peaks. The data can be fitted to the Debye model, affording α values (this parameter determines the width of the distribution of relaxation times, so that $\alpha = 1$ corresponds to an infinitely wide distribution of relaxation times, whereas $\alpha = 0$ represents a process with only a single relaxation time) between 0.34 (3.75 K) and 0.52 (9 K), which are compatible with the existence of more than one relaxation process in the whole temperature range. In the range of 3.75−6.25 K, the fit of the frequency dependence of the χ''_M signal, at each temperature, to the generalized Debye model (Figure 7) permits the relaxation times to be extracted, which are plotted as a function of $1/T$ (Figure 7, inset). The fit of the high-temperature data (5.25 to 6.25 K) to the Arrhenius law ($\tau = \tau_0 \exp(U_{eff}/k_BT)$) afforded an effective thermal energy barrier $U_{eff} = 23.8(1)$ K and with a pre-exponential factor $\tau_0 = 1.35 \times 10^{-5}$ s. This τ_0 value is much larger than expected for a SMM. This together with the fact that relaxation times deviate from

dx.doi.org/10.1021/ic402827b | Inorg. Chem. 2014, 53, 3417−3426

Table 4. Comparison of Bond Lengths (Å) and Bond Angles (deg) in the $Dy_4(\mu_3\text{-}O)_4$ Cubane Core Present in Ln_4 Complexes

	$Dy-O_{hydroxy}$	$Dy-O_{alkoxy}$	Dy−Dy	Dy−O−Dy	reference
$[Dy_4(L)_4(\mu_2\text{-}\eta^1\eta^1Piv)_2]\cdot 4H_2O\cdot 6CH_3OH$		2.36−2.49	3.68−4.15	99.20−115.10	this work
$[Dy_4(\mu_3\text{-}OH)_4(isonicotinate)_6(py)(CH_3OH)_7](ClO_4)_2\cdot py\cdot 4CH_3OH$	2.33−2.40		3.72−3.85	103.63−110.1	15a, Figure 3a
$[Dy_4(HL)_4(C_6H_4NH_2COO)_2(\mu_3\text{-}OH)_4(\mu\text{-}OH)_2(H_2O)_4]\cdot 4CH_3CN\cdot 12H_2O$[a]	2.34−2.37		3.58−3.81	99.00−109.50	15b, Figure 3b
$[Dy_4(OH)_4(TBSOC)_2(H_2O)_4(CH_3OH)_4]\cdot 4H_2O$[b]	2.33−2.36		2.57−2.73	105.7−107.9	15c, Figure 3c

[a] LH_2 = 2-{[(2-hydroxy-3-methoxyphenyl)methylidene]amino}benzoic acid. [b] (H_4TBSOC = *p-tert*-butylsulfonylcalix[4]arene).

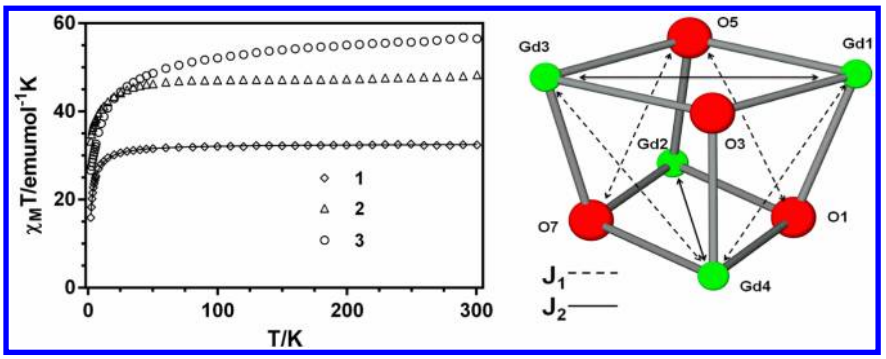

Figure 4. (left) Temperature dependence of the $\chi_M T$ for compounds **1**−**3**. Solid line represents the best fit of the experimental data. (right) 2*J* coupling scheme for compound **1**.

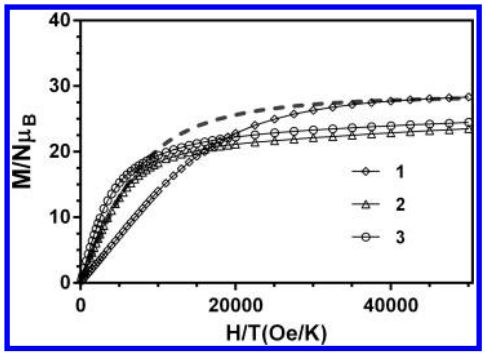

Figure 5. Field dependence of the magnetization for compounds **1**−**3**. Solid lines are just a guide to the eye. The dashed line represents the Brillouin function for four noninteracting Gd^{3+} ions.

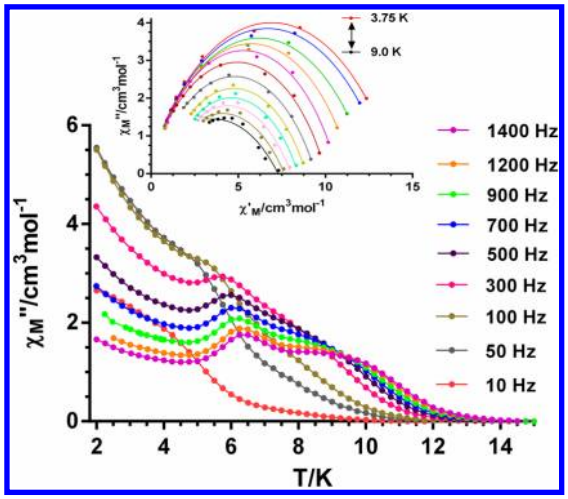

Figure 6. Temperature dependence of the out-of-phase ac signals (χ''_M) under zero applied dc field for **3**. Solid lines are a guide to the eye. (inset) Cole−Cole plot for **3**. Solid lines represent the best fitting to the Debye model.

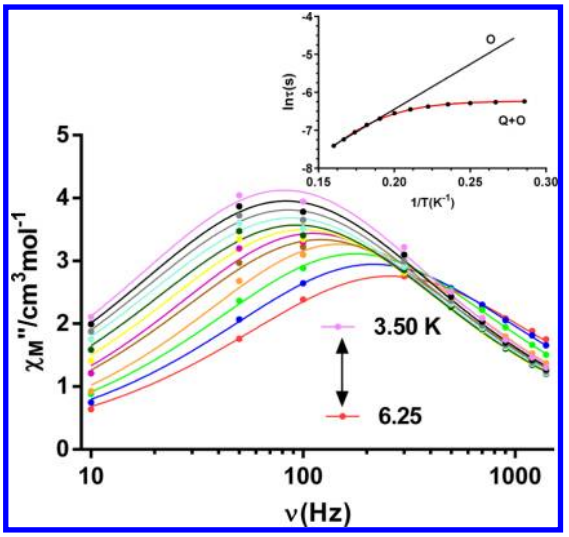

Figure 7. Frequency dependence of χ''_M for compound **3** under a zero dc field. (inset) Temperature dependence of the relaxation times for **3** under a zero dc field. (black line) The best fitting of the experimental data to the Arrhenius equation. (red line) The best fit to an Orbach and QTM process.

linearity in the low-temperature region (Figure 7) agrees with the simultaneous occurrence of both QTM and Orbach thermally activated processes. In view of this, we have fitted the temperature dependence of the relaxation time to the following equation that considers the simultaneous occurrence of both the thermal and QTM processes:

$$\tau^{-1} = \tau_{QT}^{-1} + \tau_0^{-1}\exp(-U_{eff}/kT) \quad (1)$$

An excellent fit over the full temperature range was obtained with the following parameters: U_{eff} = 43.4(9) K with $\tau_0 = 8 \times 10^{-7}$ s and τ_{QT} = 0.001 97(2) s. As expected, when the effects of the QTM process are taken into consideration, the U_{eff} and τ_0 values increase and decrease, respectively. The absence of well-separated peaks in the χ''_M versus *T* and χ''_M versus ν plots

dx.doi.org/10.1021/ic402827b | Inorg. Chem. 2014, 53, 3417−3426

prevents extraction of reliable U_{eff} and τ_0 values for the SR process.

The ac measurements, in the presence of a small external dc field of 1000 Oe (Figure 8 and Supporting Information, Figure S4) to fully or partly suppress the QTM, show that (i) the two peaks are rather well-resolved, so that maxima are clearly observed for both processes, (ii) the χ''_M signal peaks appear virtually at the same temperatures as those observed under zero dc applied field and exhibit similar intensity, and (iii) χ''_M components do not go to zero below the maxima of the FR process, which can be taken as a clear indication that the QTM process has not been efficiently suppressed. Note that position of the peaks does not significantly shift when the dc applied magnetic field is increased to 3000 Oe (Supporting Information, Figure S5). However, the peaks for the FR process increase in intensity with regard to those for the SR process. Moreover, magnetic fields as high as 3000 Oe are not able to fully eliminate the QTM relaxation process, which suggests that the remaining QTM process is promoted by intermolecular magnetic dipolar interactions. An appropriate manner to try to eliminate the intermolecular interactions and therefore the QTM process is that of diluting the sample with an isostructural diamagnetic complex, such as Y^{III}_4. These experiments are planned for the near future in case we are able to cocrystallize the Dy^{III}_4 complex with the isotructural Y^{III}_4 diamagnetic complex. In spite of this, changes occurring in the temperature and frequency dependence of the χ''_M component of the ac susceptibility make it easier to analyze the data and to extract reliable parameters for the FR and SR relaxation processes.

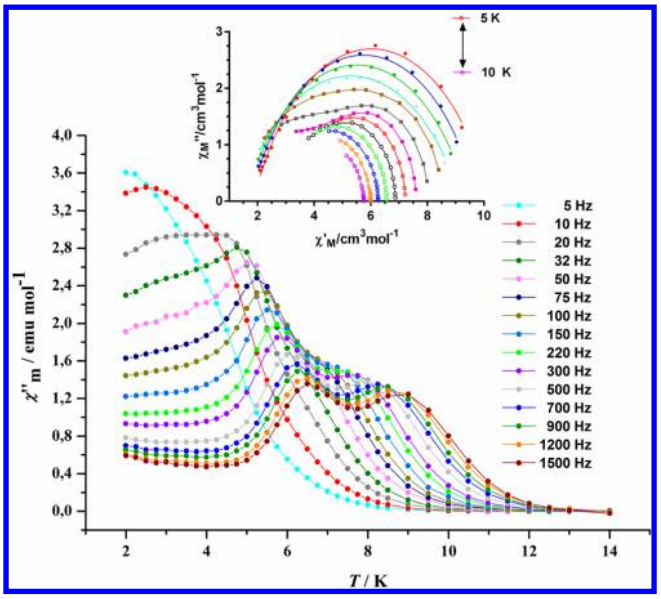

Figure 8. Temperature dependence of the out-of-phase ac signals (χ''_M) under an applied dc field of 1000 Oe for compound **3**. Solid lines are a guide to the eye. (inset) Cole−Cole plot for **3** under an applied dc field of 1000 Oe. Solid lines represent the best fitting to the Debye model.

The Cole−Cole plot, between 5 and 5.75 K, shows an almost single semicircle corresponding to the FR. However, as the temperature is increased, the FR and SR processes are both observed in the range of 6−8 K; from this latter temperature, the faster process gradually moves beyond the high-frequency range of the magnetometer (<1500 Hz), and only a semicircle due to the SR process can be observed. The fit of the data using the generalized Debye model afforded α values in the ranges of 0.34 (5.75 K)−0.26 (5 K) and 0.08 (10 K)−0.16 (8 K) for the FR and SR regions, respectively, which supports the existence of multiple relaxation processes for the former (in good accord with the ineffective suppression of the QTM) and a relatively narrow distribution of the relaxation times for the latter.

The χ''_M versus frequency curves were fitted by using the sum of two modified Debye functions[25] (Figure 9), and from the extracted relaxation times the corresponding Arrhenius plots were constructed (Figure 9 inset), which led to $\tau_0 = 2.7 \times 10^{-6}$ s and $U_{eff} = 37(1)$ K for the FR process and $\tau_0 = 4.4 \times 10^{-8}$ s and $U_{eff} = 73(2)$ K for the SR process. As observed for the relaxation times extracted at zero field for the FR process, the data at 1000 Oe also deviate from linearity in the low-temperature region, and τ_0 is much larger than expected for an SMM. Both facts point out that both QTM and Orbach thermally activated processes occur simultaneously. In fact, a good fit of the data in the 3.5−5.75 K range is obtained with 1 and the following parameters: $U_{eff} = 47.2(9)$ K with $\tau_0 = 5 \times 10^{-7}$ s and $\tau_{QT} = 0.0157(9)$ s. It seems that in the presence of an external field of 1000 Oe, the QTM is partly suppressed, but the relaxation of the magnetization does not significantly slow with regard to the same process under zero dc applied field. The Arrhenius plots, constructed from the temperatures and frequencies of the maxima observed for the χ''_M signals in Figure 8, lead virtually to the same results, as expected (see Figure S6). It is worth mentioning that the values of the effective energy barrier for the FR and SR processes in **3** are at the high end of the range found for the limited number of Dy_4 SMMs so far reported, and they are the largest values ever found for Dy_4O_4 cubane complexes. In addition, the pre-exponential factor τ_0 is typical of SMMs.[8]

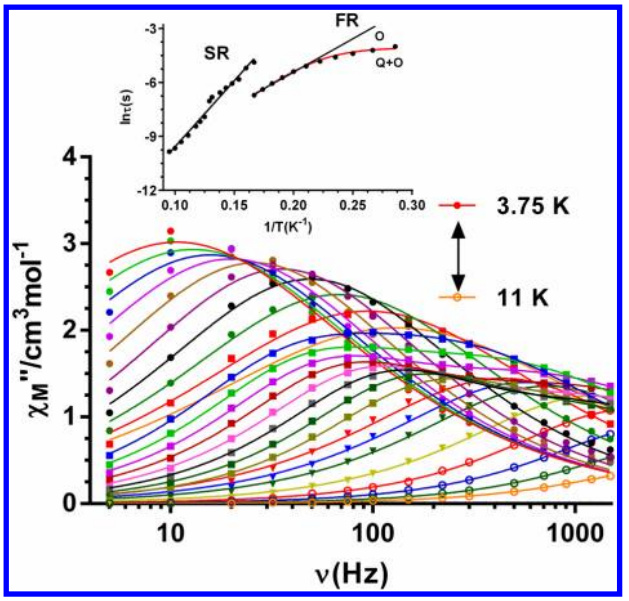

Figure 9. Frequency dependence of χ''_M for **3** under a 1000 Oe dc field. (inset) Temperature dependence of the relaxation times for **3** under an applied dc field of 1000 Oe. (black line) The best fit of the experimental data to the Arrhenius equation. (red line) The best fit to an Orbach and QTM process.

It is worth mentioning that Dy^{III}-containing polynuclear complexes usually exhibit very weak Dy···Dy exchange interactions because of the limited radial extension of their

dx.doi.org/10.1021/ic402827b | Inorg. Chem. 2014, 53, 3417−3426

inner f orbitals. Consequently, in these systems the SR of the magnetization is mainly due to the large moment and strong magnetic anisotropy of the individual Dy^{III} centers rather than to the fully exchange-coupled molecule. Therefore, polynuclear complexes can exhibit several relaxation processes corresponding to multiple slow relaxing Dy^{III} centers. In the absence of significant magnetic exchange coupling between the Dy^{III} ions, the relaxation of the individual ions allows for the occurrence of QTM at zero applied field. It has been shown that significant exchange coupling between the Dy^{III} ions mitigates the QTM process.[26] In view of the above results for the Gd^{III} complex **1**, the Dy···Dy exchange interactions in **3** are expected to be very weak, and therefore the relaxation process should have a single-ion origin with QTM at zero field. The existence of a tail at low temperature and zero applied field in the χ''_M versus T plot of **3** could support this assumption. Assuming the single-ion origin of the magnetic relaxation in **3**, the existence of two thermally activated relaxation processes could be due to (i) the noncrystallographic equivalence of the four Dy^{III} ions with small differences between distances and angles in their corresponding DyO_8 coordination polyhedra and (ii) the existence of two competing relaxation pathways via excited states, which depends on the transverse field each Dy^{III} ion experiences from its neighboring Dy^{III} ions.[11]

CONCLUSIONS

To summarize, we report the synthesis and the structural and magnetic characterization of tetranuclear lanthanide complexes having a distorted cubane-type tetrametallic core. The assembly of these complexes has been accomplished by the use of a semiflexible unsymmetrical Schiff-base ligand containing a distinct binding pocket for lanthanide metal ions. However, the deprotonated $(-CH_2O)^-$ arm of the ligand along with the ancillary pivalate ions allows the assembly to proliferate. The magnetic studies involving the ac susceptibility measurements reveal that among compounds **1**, **2**, and **3**, only compound **3** exhibits an SR of magnetization below 10 K. This compound shows two relaxation processes that lead to two energy barriers (73 and 47 K) and time constants ($\tau_0 = 4.4 \times 10^{-8}$ s, $\tau_0 = 5.0 \times 10^{-7}$ s).

ASSOCIATED CONTENT

Supporting Information

Molecular structures of **1** and **2**, details of structural parameters for compounds **1** and **2**, and magnetic data for **3**. This material is available free of charge via the Internet at http://pubs.acs.org. Crystallographic data (excluding structure factors) for the structures in this Paper have been deposited with the Cambridge Crystallographic Data Centre as supplementary publication Nos. CCDC 963386−963388. Copies of the data can be obtained, free of charge, on application to CCDC, 12 Union Road, Cambridge CB2 1EZ, U.K.: http://www.ccdc.cam.ac.uk/cgi-bin/catreq.cgi, e-mail: data_request@ccdc.cam.ac.uk, or fax: +44 1223 336033.

AUTHOR INFORMATION

Corresponding Authors

*E-mail: vc@iitk.ac.in. (V.C.)
*E-mail: ecolacio@ugr.es. (E.C.)

Notes

The authors declare no competing financial interest.

ACKNOWLEDGMENTS

We are thankful to the Department of Science and Technology, New Delhi, for financial support. S.D., A.D., and S.B. thank CSIR, India for Senior Research Fellowship. V.C. is thankful to the Department of Science and Technology (DST) for a J. C. Bose National Fellowship. E.C. is thankful for financial support from the Spanish Ministerio de Ciencia e Innovación (MICINN) (Project CTQ-2011-24478), the Junta de Andalucía (FQM-195, the Project of Excellence P11-FQM-7756), and the University of Granada. We are grateful to Nuria Clos, Unitat de Mesures Magnètiques, Centers Cinetifics i Tecnològics, Universitat de Barcelona, Spain, for his help with the magnetic measurements.

REFERENCES

(1) (a) Christou, G.; Gatteschi, D.; Hendrickson, D. N.; Sessoli, R. *Mater. Res. Bull.* **2000**, *25*, 66−71. (b) Sessoli, R.; Gatteschi, D.; Caneschi, A.; Novak, M. A. *Nature* **1993**, *365*, 141−143. (c) Affronte, M. *J. Mater. Chem.* **2009**, *19*, 1731−1737. (d) Stamp, P. C. E.; Gaita-Arino, A. *J. Mater. Chem.* **2009**, *19*, 1718−1730. (e) Aromı, G.; Aguila, D.; Gamez, P.; Luis, F.; Roubeau, O. *Chem. Soc. Rev.* **2012**, *41*, 537−546. (f) Ardavan, A.; Rival, O.; Morton, J. J. L.; Blundell, S. J.; Tyryshkin, A. M.; Timco, G. A.; Winpenny, R. E. P. *Phys. Rev. Lett.* **2007**, *98*, 057201−057204. (g) Bogani, L.; Wernsdorfer, W. *Nat. Mater.* **2008**, *7*, 179−186. (h) Leuenberger, M. N.; Loss, D. *Nature* **2001**, *410*, 789−793.

(2) (a) Peng, J. B.; Zhang, Q. C.; Kong, X. J.; Ren, Y. P.; Long, L. S.; Huang, R. B.; Zheng, L. S.; Zheng, Z. P. *Angew. Chem., Int. Ed.* **2011**, *50*, 10649−10652. (b) Zheng, Y. Z.; Evangelisti, M.; Winpenny, R. E. P. *Angew. Chem., Int. Ed.* **2011**, *50*, 3692−3695. (c) Liu, S.-J.; Zhao, J.-P.; Tao, J.; Jia, J.-M.; Han, S.-D.; Li, Y.; Chen, Y.-C.; Bu, X.-H. *Inorg. Chem.* **2013**, *52*, 9163−9698. (d) Biswas, S.; Adhikary, A.; Goswami, S.; Konar, S. *Dalton Trans.* **2013**, *42*, 13331−13334.

(3) (a) Mannini, M.; Pineider, F.; Danieli, C.; Totti, F.; Sorace, L.; Sainctavit, P.; Arrio, M. A.; Otero, E.; Joly, L.; Cezar, J. C.; Cornia, A.; Sessoli, R. *Nature* **2010**, *468*, 417−421. (b) Bokacheva, L.; Kent, A. D.; Walters, M. A. *Phys. Rev. Lett.* **2000**, *85*, 4803−4806. (c) Hill, S.; Edwards, R. S.; Aliaga-Alcalde, N.; Christou, G. *Science* **2003**, *302*, 1015−1018. (d) Friedman, J. R.; Patel, V.; Chen, W.; Tolpygo, S. K.; Lukens, J. E. *Nature* **2000**, *406*, 43−46.

(4) (a) Aromi, O. G.; Brechin, E. K. *Struct. Bonding (Berlin, Ger.)* **2006**, *122*, 1−67. (b) Sessoli, R.; Powell, A. K. *Coord. Chem. Rev.* **2009**, *253*, 2328−2341.

(5) (a) Gatteschi, D.; Sessoli, R.; Villain, J. *Molecular Nanomagnets;* Oxford University Press: Oxford, 2006. (b) Sessoli, R.; Hui, L.; Schake, A. R.; Wang, S.; Vincent, J. B.; Folting, K.; Gatteschi, D.; Christou, G. *J. Am. Chem. Soc.* **1993**, *115*, 1804−1816.

(6) Ako, A. M.; Hewitt, I. J.; Mereacre, V.; Clérac, R.; Wernsdorfer, W.; Anson, C. E.; Powell, A. K. *Angew. Chem., Int. Ed.* **2006**, *45*, 4926−4929.

(7) Ako, A. M.; Mereacre, V.; Clérac, R.; Wernsdorfer, W.; Hewitt, I. J.; Anson, C. E.; Powell, A. K. *Chem. Commun.* **2009**, 544−546.

(8) Woodruff, D. N.; Winpenny, R. E. P.; Layfield, R. A. *Chem. Rev.* **2013**, *113*, 5110−5148 and references therein.

(9) (a) Ishikawa, N.; Sugita, M.; Ishikawa, T.; Koshihara, S.-y.; Kaizu, Y. *J. Am. Chem. Soc.* **2003**, *125*, 8694−8695. (b) Ishikawa, N.; Sugita, M.; Wernsdorfer, W. *J. Am. Chem. Soc.* **2005**, *127*, 3650−3651. (c) Fatila, E. M.; Rouzières, M.; M. Jennings, C. A.; Lough, J.; Clérac, R.; Preuss, K. E. *J. Am. Chem. Soc.* **2013**, *135*, 9596−9599. (d) Liu, C.-M.; Zhang, D.-Q.; Zhu, D.-B. *Inorg. Chem.* **2013**, *52*, 8933−8940. (e) Campbell, V. E.; Guillot, R.; Riviere, E.; Brun, P.-T.; Wernsdorfer, W.; Mallah, T. *Inorg. Chem.* **2013**, *52*, 5194−5200.

(10) Blagg, R. J.; Muryn, C. A.; McInnes, E. J. L.; Tuna, F.; Winpenny, R. E. P. *Angew. Chem., Int. Ed.* **2011**, *50*, 6530−6533.

(11) Blagg, R. J.; Ungur, L.; Tuna, F.; Speak, J.; Comar, P.; Collison, D.; Wernsdorfer, W.; McInnes, E. J. L.; Chibotaru, L. F.; Winpenny, R. E. P. *Nat. Chem.* **2013**, *5*, 673−678.

(12) (a) Chandrasekhar, V.; Hossain, S.; Das, S.; Biswas, S.; Sutter, J. P. *Inorg. Chem.* **2013**, *52*, 6346−6353. (b) Chandrasekhar, V.; Bag, P.; Colacio, E. *Inorg. Chem.* **2013**, *52*, 4562−4570. (c) Chandrasekhar, V.; Dey, A.; Mota, A. J.; Colacio, E. *Inorg. Chem.* **2013**, *52*, 4554−4561. (d) Chandrasekhar, V.; Das, S.; Dey, A.; Hossain, S.; Sutter, J.-P. *Inorg. Chem.* **2013**, *52*, 11956−11965.

(13) (a) Chandrasekhar, V.; Pandian, B. M.; Azhakar, R.; Vittal, J. J.; Clérac, R. *Inorg. Chem.* **2007**, *46*, 5140−5142. (b) Chandrasekhar, V.; Pandian, B. M.; Vittal, J. J.; Clérac, R. *Inorg. Chem.* **2009**, *48*, 1148−1157. (c) Chandrasekhar, V.; Dey, A.; Das, S.; Rouziéres, M.; Clérac, R. *Inorg. Chem.* **2013**, *52*, 2588−2598. (d) Chandrasekhar, V.; Bag, P.; Speldrich, M.; Leusen, J.; Kögerler, P. *Inorg. Chem.* **2013**, *52*, 5035−5044. (e) Chandrasekhar, V.; Das, S.; Dey, A.; Hossain, S.; Lloret, F.; Pardo, E. *Eur. J. Inorg. Chem.* **2013**, 4506−4514.

(14) (a) Petit, S.; Neugebauer, P.; Pilet, G.; Chastanet, G.; Barra, A.-L.; Antunes, A. B.; Wernsdorfer, W.; Luneau, D. *Inorg. Chem.* **2012**, *51*, 6645−6654. (b) Papadakis, R.; Rivière, E.; Giorgi, M.; Jamet, H.; Rousselot-Pailley, P.; Réglier, M.; Simaan, A. J.; Tron, T. *Inorg. Chem.* **2013**, *52*, 5824−5830. (c) Guedes, G. P.; Soriano, S.; Comerlato, N. M.; Speziali, N. L.; Lahti, P. M.; Novak, M. A.; Vaz, M. G. F. *Eur. J. Inorg. Chem.* **2012**, 5642−5648. (d) Oshio, H.; Hoshino, N.; Ito, T.; Nakano, M. *J. Am. Chem. Soc.* **2004**, *126*, 8805−8812. (e) Piga, F.; Moro, F.; Krivokapic, I.; Blake, A. J.; Edge, R.; McInnes, E. J. L.; Evans, D. J.; McMastera, J.; Slageren, J. v. *Chem. Commun.* **2012**, *48*, 2430−2432. (f) Moragues-Canovas, M.; Helliwell, M.; Ricard, L.; Riviere, E.; Wernsdorfer, W.; Brechin, E.; Mallah, T. *Eur. J. Inorg. Chem.* **2004**, 2219−2222. (g) Yang, E. C.; Wernsdorfer, W.; Zakharov, L. N.; Karaki, Y.; Yamaguchi, A.; Isidro, R. M.; Lu, G. D.; Wilson, S. A.; Rheingold, A. L.; Ishimoto, H.; Hendrickson, D. N. *Inorg. Chem.* **2006**, *45*, 529−546. (h) Galloway, K. W.; Whyte, A. M.; Wernsdorfer, W.; Sanchez-Benitez, J.; Kamenev, K. V.; Parkin, A.; Peacock, R. D.; Murrie, M. *Inorg. Chem.* **2008**, *47*, 7438−7442. (i) Isele, K.; Gigon, F.; Williams, A. F.; Bernardinelli, G.; Franz, P.; Decurtins, S. *Dalton Trans.* **2007**, 332−341. (j) Venegas-Yazigi, D.; Cano, J.; Ruiz, E.; Alvarez, S. *Phys. Rev. B: Condens. Matter Mater. Phys.* **2006**, *384*, 123−125. (k) Gao, Y.; Zhao, L.; Xu, X.; Xu, G.-F.; Guo, Y.-N.; Tang, J.; Liu, Z. *Inorg. Chem.* **2011**, *50*, 1304−1308. (l) Aronica, C.; Chastanet, G.; Pilet, G.; Le Guennic, B.; Robert, V.; Wernsdorfer, W.; Luneau, D. *Inorg. Chem.* **2007**, *46*, 6108−6119. (m) Zhao, X. Q.; Lan, Y. H.; Zhao, B.; Cheng, P.; Anson, C. E.; Powell, A. K. *Dalton Trans.* **2010**, *39*, 4911−4917. (n) Nohra, B.; Mialane, P.; Dolbecq, A.; Riviere, E.; Marrot, J.; Secheresse, F. *Chem. Commun.* **2009**, 2703−2711. (o) Das, A.; Klinke, F. J.; Demeshko, S.; Meyer, S.; Dechert, S.; Meyer, F. *Inorg. Chem.* **2012**, *51*, 8141−8149. (p) Yang, E.-C.; Wernsdorfer, W.; Hill, S.; Edwards, R. S.; Nakano, M.; Maccagnano, S.; Zakharov, L. N.; Rheingold, A. L.; Christou, G.; Hendrickson, D. N. *Polyhedron* **2003**, *22*, 1727−1733.

(15) (a) Gao, Y. J.; Xu, G. F.; Zhao, L.; Tang, J.; Liu, Z. L. *Inorg. Chem.* **2009**, *48*, 11495−11497. (b) Ke, H. S.; Gamez, P.; Zhao, L.; Xu, G. F.; Xue, S. F.; Tang, J. *Inorg. Chem.* **2010**, *49*, 7549−7557. (c) Liu, C.-M.; Zhang, D.-Q.; Hao, X.; Zhu, D.-B. *Cryst. Growth Des.* **2012**, *12*, 2948−2954. (d) Chesman, A. S. R.; Turner, D. R.; Moubaraki, B.; Murray, K. S.; Deacon, G. B.; Batten, S. R. *Dalton Trans.* **2012**, *41*, 3751−3757. (e) Savard, D.; Lin, P.-H.; Burchell, T. J.; Korobkov, I.; Wernsdorfer, W.; Clérac, R.; Murugesu, M. *Inorg. Chem.* **2009**, *48*, 11748−11754. (f) Kong, X.-J.; Long, L.-S.; Zheng, L.-S.; Wang, R.; Zheng, Z. *Inorg. Chem.* **2009**, *48*, 3268−3273. (g) Gerasko, O. A.; Mainicheva, E. A.; Naumova, M. I.; Yurjeva, O. P.; Alberola, A.; Vicent, C.; Llusar, R.; Fedin, V. P. *Eur. J. Inorg. Chem.* **2008**, 416−424. (h) Ma, B.-Q.; Zhang, D.-S.; Gao, S.; Jin, T.-Z.; Yan, C.-H.; Xu, G.-X. *Angew. Chem., Int. Ed.* **2000**, *39*, 3644−3646. (i) Baskar, V.; Roesky, P. W. *Dalton Trans.* **2006**, 676−679. (j) Zheng, Z. P. *Chem. Commun.* **2001**, 2521−2529. (k) Kong, X. J.; Wu, Y. L.; Long, L. S.; Zheng, L. S.; Zheng, Z. P. *J. Am. Chem. Soc.* **2009**, *131*, 6918−6919.

(16) Furniss, B. S.; Hannaford, A. J.; Smith, P. W. G.; Tatchell, A. R. *Vogel's Textbook of Practical Organic Chemistry,* 5th ed.; ELBS, Longman: London, 1989.

(17) (a) Ziessel, R.; Nguyen, P.; Douce, L.; Cesario, M.; Estournes, C. *Org. Lett.* **2004**, *6*, 2865−2868. (b) Artali, R.; Botta, M.; Cavallotti, C.; Giovenzana, G. B.; Palmisano, G.; Sisti, M. *Org. Biomol. Chem.* **2007**, *5*, 2441−2447. (c) Hutchinson, D. J.; Hanton, L. R.; Moratti, S. C. *Inorg. Chem.* **2010**, *49*, 5923−5934.

(18) (a) *SMART & SAINT Software Reference manuals,* Version 6.45; Bruker Analytical X-ray Systems, Inc.: Madison, WI, 2003. (b) Sheldrick, G. M. *SADABS,* a software for empirical absorption correction, Ver. 2.05; University of Göttingen: Göttingen, Germany, 2002. (c) *SHELXTL Reference Manual,* Ver. 6.1; Bruker Analytical X-ray Systems, Inc.: Madison, WI, 2000. (d) Sheldrick, G. M. *SHELXTL,* Ver. 6.12; Bruker AXS, Inc.: Madison, WI, 2001. (e) Sheldrick, G. M. *SHELXL97, Program for Crystal Structure Refinement*; University of Göttingen: Göttingen, Germany, 1997. (f) Bradenburg, K. *Diamond,* Ver. 3.1eM; Crystal Impact GbR: Bonn, Germany, 2005.

(19) (a) Abbas, G.; Lan, Y.; Kostakis, G. E.; Wernsdorfer, W.; Anson, C. E.; Powell, A. K. *Inorg. Chem.* **2010**, *49*, 8067−8072. (b) Abbas, G.; Lan, Y.; Kostakis, G.; Anson, C. E.; Powell, A. K. *Inorg. Chim. Acta* **2008**, *361*, 3494−3499. (c) Liu, S.-J.; Zhao, J.-P.; Song, W.-C.; Han, S.-D.; Liu, Z.-Y.; Bu, X.-H. *Inorg. Chem.* **2013**, *52*, 2103−2109. (d) Langley, S. K.; Chilton, N. F.; Gass, I. A.; Moubaraki, B.; Murray, K. S. *Dalton Trans.* **2011**, *40*, 12656−12659. (e) Mereacre, V.; Prodius, D.; Lan, Y. H.; Turta, C.; Anson, C. E.; Powell, A. K. *Chem.—Eur. J.* **2011**, *17*, 123−128. (f) Rinck, J.; Novitchi, G.; Heuvel, W. V. D.; Ungur, L.; Lan, Y. H.; Wernsdorfer, W.; Anson, C. E.; Chibotaru, L. F.; Powell, A. K. *Angew. Chem., Int. Ed.* **2010**, *49*, 7583−7587. (g) Zheng, Y. Z.; Evangelisti, M.; Winpenny, R. E. P. *Angew. Chem., Int. Ed.* **2011**, *50*, 3692−3695.

(20) (a) Alvarez, S.; Alemany, P.; Casanova, D.; Cirera, J.; Llunell, M.; Avnir, D. *Coord. Chem. Rev.* **2005**, *249*, 1693−1780. (b) Casanova, D.; Llunell, M.; Alemany, P.; Alvarez, S. *Chem.—Eur. J.* **2005**, *11*, 1479−1494.

(21) MAGMUN 4.0/OW0L is available as a combined package free of charge from the authors at http://www.ucs.mun.ca/lthomp/. MAGMUN has been developed by Dr. Xu, Z. and Thompson, L. K. (Memorial University), and OW01.exe was developed by Dr. Waldmann, O. (University of Bern). The software calculates the total spin state values (*S*) and their associated energies (*E*), using the Kambe approach, and then substitutes the *S* and *E* values into the van Vleck equation to generate the variable-temperature susceptibility profile (degenerate states are accounted for).

(22) (a) Costes, J. P.; Dupuis, A.; Laurent, J. P. *Inorg. Chim. Acta* **1998**, *268*, 125−130. (b) John, D.; Urland, W. *Eur. J. Inorg. Chem.* **2006**, 3503−3509 and references therein. (c) Avecilla, F.; Platas-Iglesias, C.; Rodríguez-Cortiñas, R.; Guillemot, G.; Bünzli, J. C. G.; Brondino, C. D.; Geraldes, C. F. G. C.; de Blas, A.; Rodríguez-Blas, T. *J. Chem. Soc., Dalton Trans.* **2002**, 4658−4665. (d) Long, J.; Habib, F.; Lin, P.-H.; Korobkov, I.; Enright, G.; Ungur, L.; Wernsdorfer, W.; Chibotaru, L. F.; Murugesu, M. *J. Am. Chem. Soc.* **2011**, *133*, 5319−5328.

(23) Colacio, E.; Ruiz, J.; Mota, A. J.; Palacios, M. A.; Cremades, E.; Ruiz, E.; White, F. J.; Brechin, E. K. *Inorg. Chem.* **2012**, *51*, 5857−5858.

(24) Ruiz, J.; Mota, A. J.; Rodríguez-Diéguez, A.; Titos, S.; Herrera, J. M.; Ruiz, E.; Cremades, E.; Costes, J. P.; Colacio, E. *Chem Commun.* **2012**, *48*, 7916−7918 and references therein.

(25) Domingo, N.; Luis, F.; Nakano, M.; Munto, M.; Gómez, J.; Chaboy, J.; Ventosa, N.; Campo, J.; Veciana, J.; Ruiz-Molina, D. *Phys. Rev. B* **2009**, *79*, 214404−214409.

(26) (a) Long, J.; Habib, F.; Lin, P.-H.; Korobkov, I.; Enright, G.; Ungur, L.; Wernsdorfer, W.; Chibotaru, L. F.; Murugesu, M. *J. Am. Chem. Soc.* **2011**, *133*, 5319−5328. (b) Rinehart, J. D.; Fang, M.; Evans, W. J.; Long, J. R. *Nat. Chem.* **2011**, *3*, 538−542. (c) Demir, S.; Zadrozny, J. M.; Nippe, M.; Long, J. R. *J. Am. Chem. Soc.* **2012**, *134*, 18546−18549.